Tsunami impact assessment for low-lying cities along the Northern Atlantic Coast of Morocco using MIRONE software

Abdelkarim Tadibaght, Abdelmounim El M'rini, Lionel Siame, Olivier Bellier

Tsunami impact assessment for low-lying cities along the Northern Atlantic coast of Morocco using MIRONE software

Abdelkarim TADIBAGHT[a*], Abdelmounim EL M'RINI[a], Lionel SIAME[b], Olivier Bellier[b,c]

[a] LR3G, FS, Abdelmalek Essaadi University, Tetouan, Morocco

[b] Aix Marseille Univ, CNRS, IRD, INRAE, Coll France, CEREGE, Aix-en-Provence, France

[c] Aix Marseille Univ, CNRS, ECCOREV, Aix-en-Provence, France

[*] Address correspondence to: Abdelkarim Tadibaght

E-mail: tadibaghtabde@gmail.com

Tel.: +212657966260

Abdelkarim Tadibaght Orcid: https://orcid.org/0000-0001-7161-0154

Abdelmounim El M'rini Orcid: https://orcid.org/0000-0002-7963-5660

Lionel Siame Orcid: https://orcid.org/0000-0002-4288-9528

Olivier Bellier Orcid: https://orcid.org/0000-0002-3213-7306

Abstract:

The Northern Atlantic coastline of Morocco is potentially exposed to tsunamis, like that triggered by the large Lisbon event (November 1st, 1755), also known as the most destructive event in Moroccan history. In this work, we used MIRONE software to simulate tsunami phenomenon in the Southwest Iberian Margin region, combining a series of bathymetric and topographic grid layers with an initial water elevation generated using Mansinha's formulations and assuming an instantaneous seabed movement. For this investigation, we considered four scenarios, associated with four potential seismic sources for the 1755 earthquake located in the Gulf of Cadiz. Thus, for each scenario, we obtained a map showing the results of the simulation (distance traveled, wave displacement speed, evolution of wave heights from offshore to coastal areas and arrival travel times). These maps showed that cities like Mohammedia, Casablanca and El-Jadida, were important stakes that could be impacted by a tsunami originating from these sources. For these cities, we thus determined the traveling water columns and the inland distances that could be reached by this inundation. The results show that these cities are potentially threaten by maximum water elevation exceeding 20 m in some locations, with a worse scenario characterized by flow depth and inundation distance ranging from 6 m to 10, and 1.8 km to 4.6 km, respectively. These results should also be useful for the authorities, emergency, and decision planners to develop tsunami protection and risk awareness among the coastal communities of Morocco.

Keywords: 1755 Lisbon tsunami, Numerical modeling, MIRONE, Northern Atlantic coast, Morocco.

1. Introduction

Coastal areas are exposed to quite a lot of natural hazards, from waves triggered by earthquake or extreme weather events to erosion including landslides. This situation is likely to increase in the context of global warming and sea-level rise combined to socio-economic growths, and seriously questions the adaptation of heavily urbanized areas located at low elevation. Within this context, there is a dire need to better characterize coastal hazards and associated risks located along the margin of the diffuse tectonic boundary accommodating the convergence between the Nubia and Iberia plates (Fig. 1). The Atlantic coast of Morocco is potentially threatened by tsunami waves trigged by earthquakes generated within the Gulf of Cadiz. Indeed, to the southwest of Cape Saint Vincent, oceanic earthquakes may be tsunamigenic, and generate waves that can reach the coasts of Portugal, Spain and Morocco, like during the so-called Lisbon event on November 1st, 1755 (M_W~8.5) (Solares et al., 1979; Johnston, 1996; Gutscher, 2004; Gutscher et al., 2006). The Atlantic coast of Morocco also gathers about 10.3 millions of inhabitants (Laouina, 2019), which corresponds to 33% of the total country

population according to last general population and housing census data (H.C.P, 2014). This region has always been an important attraction hub for population coming from the interior regions (El Mrini, 2011). This region also hosts some of the largest cities with a heavy weight in the Moroccan economy: Tangier, Larache, Kenitra, Rabat, Mohammedia, Casablanca and El-Jadida. In fact, accounting for all the socio-economic assets, this coveted coastline is a structuring pole of the Moroccan economy (D.A.T, 2017), which therefore experiences significant forms of pressure. It is the site of a strong land speculation and anarchic urbanization, as a consequence of important industrialization, logistics and tourist development projects, in addition to fishery and agricultural activities (Laouina, 2019). On an area of approximately 25,000 km², corresponding to the tape ~10 km from the Atlantic shores, the average density is roughly 407 inhabitants / km², almost ten times the national value (Fig. 1) (Laouina, 2019). Since the early 2000s, Morocco has implemented a strategy for the development of tourism, through the Azur plans "vision 2010" and "vision 2020". These programs being essentially based on the development of coastal tourism, several resorts and hotel structures have thus been constructed along the coastlines concerned by this study. So, the combination of the Moroccan coast's exposition to the tectonic setting in the Gulf of Cadiz with density of population and economic assets should thus be an important motivation for adequately managing this region for protection against natural coastal hazards.

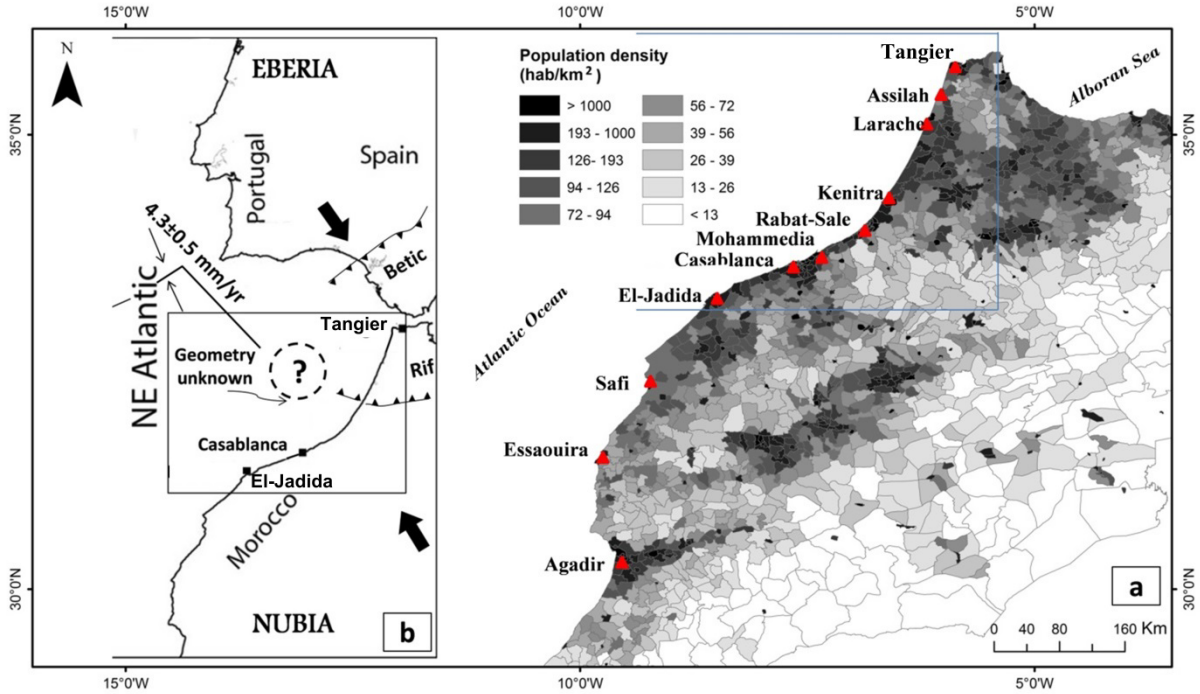

Figure 1: (a) Map of the study area showing the population density and the principal cities of Northern Morocco (based on Laouina, 2019), (b) tectonic boundary and regional overview of the Northeast Atlantic area.

In this work, our aim is to identify high-risk cities for tsunamis events using open-source models where quantitative assessments should also be carried out *(e.g.*, Tadibaght et al., 2022). In this study, tsunami characteristics such as inundation boundaries, flow depths, inundation distance, and inundation areas were simulated (for some of the largest socio-economical areas) along the Atlantic coast of Morocco, allowing for a regional reappraisal of the tsunami risk assessment. Considering several potential earthquake sources located in the Gulf of Cadiz, and using MIRONE code (Luis, 2007), this characterization is achieved through a scenario-based approach like that described *in* Omira et al. (2009), which considers an initial sea-surface perturbation created by an instantaneous seabed displacement (*e.g.*, Mansinha and Smylie, 1971). It was executed on a series of bathymetric and topographic grid layers (300 m, 60 m, 15 m, 10 m and 2 m resolutions). The results are displayed as maps of Maximum Flow (Depth and Distance), and Maximum Wave Elevation from epicenter to the coast for the more exposed cities along the coast and discussed regarding historical data and previously published models.

2. Extreme coastal events and geodynamic setting of the Gulf of Cadiz region

Tsunamis generally comprise a series of superficial oceanic waves generated for example by a volcanic eruption, an earthquake, or a submarine landslide, and spread in the ocean at high speed together with a relatively small amplitude. Approaching coastal areas, the wave speed decreases while the amplitude increases in response to the spatial compression due to the shallowing bathymetry. When exceeding tens of meters, such coastal waves can drown large areas of low-lying regions like during the 2004 Sumatra (Chadha et al., 2005) and the 2011 Tohoku-oki (Goto et al., 2014) events. Most of large tsunamis are generally associated with high magnitude ($M_w \geq 8.5$) earthquakes along subduction zones (*e.g.,* Jing et al., 2013).

Offshore of the Atlantic coasts of Morocco, the Southwestern Iberian margin region is characterized by submarine faults that are considered capable to release energy similar to that of a subduction zone (Gutscher et al., 2006). Around the Gulf of Cadiz, the countries that are exposed to potential tsunami events are Portugal, Spain, and Morocco (Fig. 1). The earthquake that caused the Lisbon catastrophe in 1755 also triggered a transoceanic tsunami (Roger et al., 2010a, 2010b, and 2011) that was observed in most of countries of the Northern Atlantic Ocean, with major repercussions along the coastlines of Portugal, southwest Spain and Northern Morocco (Solares et al., 1979; Johnston, 1996; Baptista et al., 1998; Gutscher et al., 2006). In the

archives, historians described this tsunami and its consequences on European and Moroccan coasts, suggesting that its main source was a strong earthquake in the southwestern Iberian margin region. Nonetheless, the understanding of this tsunami is still debated and imposes a confrontation of the historical sources in terms of interpretation, since some parameters such as the actual location of the seismic epicenter, the height of waves or, the flooded zones are not well known (*e.g.,* Baptista et al., 1998; Omira et al., 2009). However, some studies suggested that the seismogenic source of the 1755 and 1969 (Mw=7.8) events could be the same (Levret, 1991). Mentioning a great impact of the 1755 tsunami along the Moroccan shores, Soyris (1755) described tsunami wave height of 24 m and run-ups reaching about 15 m (Blanc, 2008). Barkan et al. (2009) reported that the run-up of this tsunami has reached 5 to 15 m along the Moroccan and Portuguese coasts. Therefore, the 1969 event is also worth mentioning in terms of the need to evacuate the shore-dwelling population as the Casablanca tide gauge recorded the first wave of tsunami which peaking at about 0.8 m (Gjevik et al., 1997). There are other tsunami sources like the November 1941 tsunami event which had its epicenter along the Gloria fault (Baptista et al., 2020) and that was recorded in several locations along the Moroccan coast with a maximum wave's amplitude reach up to 0.25 m in Casablanca and 0.45 m in Essaouira (Kaabouben et al., 2009). However, tsunami simulations for the 1941 event, including some Moroccan coastal areas, done a maximum wave's amplitude reach up to 0.09 m and 0.12 m respectively (Baptista et al., 2016). More recently, some seismic events occurred with lower magnitude in 2003 (Mw= 5.3), 2007 (Mw = 5.9) and 2009 (Mw=5.5), without triggering tsunamis (Pro et al., 2013). However, Omira et al. (2012), using tsunami simulations, showed that the descriptions included in the historical archives may overestimate the tsunami characteristics. In addition, geomorphic and sedimentological markers of coastal extreme events have been described along the coasts of Portugal (Algarve: Andrade, 1992); (Lisbon: Scheffers and Kelletat, 2005); (Cascais-Caboda Roca: Oliveira et al., 2011), Spain (Cadiz: Dabrio et al., 1998; Luque et al., 2001); (Cabo of Trafalgar: Whelan and Kelletat, 2005), and Morocco (Tangier: El Talibi et al., 2021, Rabat: Medina et al., 2011; Mhammdi et al., 2008, Loukkos zone: Mhammdi and Medina, 2015). However, the origin of the triggering waves is still largely debated between tsunami or strong storm events (Scheffers, 2002; Hall et al., 2008; Morton et al., 2008; Goff et al., 2009, 2012b; Switzer and Burston, 2010; Hoffmann et al., 2013). It should be mentioned that there are other studies on coastal geomorphology and sedimentology of tidal ranges and different energy systems (*e.g.,* Dill and Kaufhold, 2018; Dill et al., 2020), which it can used with others like sedimentological, chemical and mineralogical approaches to find out the origin of recent or historiques events deposits and landforms (*e.g.,* Dill, 2022). This leads us to distinguish each phenomenon from another (i.e., storms or tsunamis), as was done exactly in a research paper by

Ruiz Muñoz et al., 2021, where a set of the easternmost mineralogical and geochemical evidence of the 1755 Lisbon tsunami event were found in the Western Mediterranean.

The studied area comprises large Moroccan cities between Tangier and El-Jadida along the Northern Atlantic coast of Morocco, which are potentially exposed to tsunami impact generated by earthquakes occurring in the Southwestern Iberian margin region (*e.g.,* Blanc, 2009, 2008). In this region, a complex of faults is located at the end of the eastern Azores-Gibraltar plate boundary that separates the Nubian and Iberia continental plates. Along the Azores-Gibraltar plate boundary, the deformation pattern changes from ENE-WSW extension, close to the Azores triple junction to right lateral strike slip along the Gloria fault and compressional deformation from the Gorringe Bank through the Alboran Sea (*e.g.,* Hayward et al., 1999) (Fig. 2). This area is tectonically active and produced tsunamis generated by a number of earthquakes (*e.g.,* Baptista et al., 1998), like 1755 November 1st (Gutscher et al., 2006), 1941 November 25th (Mw 8) (Buforn et al., 1988,2004), 1969 February 28th (Mw 7.3), 1975 May 26th (Mw7.9), and 2007 February12th (Mw 6.3) (Baptista et al., 1992; Heinrich et al., 1994). In this region, the main active structures are the Marquês do Pombal Fault (Zitellini et al., 1999), Gorringe Bank Fault (Johnston, 1996), Portimão Bank Fault (Zitellini et al., 2009; Lima et al., 2010), Gulf of Cádiz Fault (Gutscher et al., 2002; Gutscher et al., 2006), and Horseshoe Fault (Gracia et al., 2003). Even if the source of the Lisbon event is still debated, Johnston (1996) suggested that its origin zone may well be a structure located between the Coral Patch Ridge and the Gorringe Bank (Fig. 2). Recent studies based on seismic reflection and multibeam echosounder data indicated that three major faults can be possibly the source of 1755 event: the N60°E-striking thrust Gorringe Bank Fault (Johnston, 1996; Grandin et al., 2007), the NNE, trending Marquês do Pombal thrust fault (Zitellini et al., 2001; Gracia et al., 2003), and the western Gulf of Cádiz Fault, possibly as part of an Nubian plate subduction beneath Gibraltar (Gutscher et al., 2002; 2006; Thiebot and Gutscher, 2006).

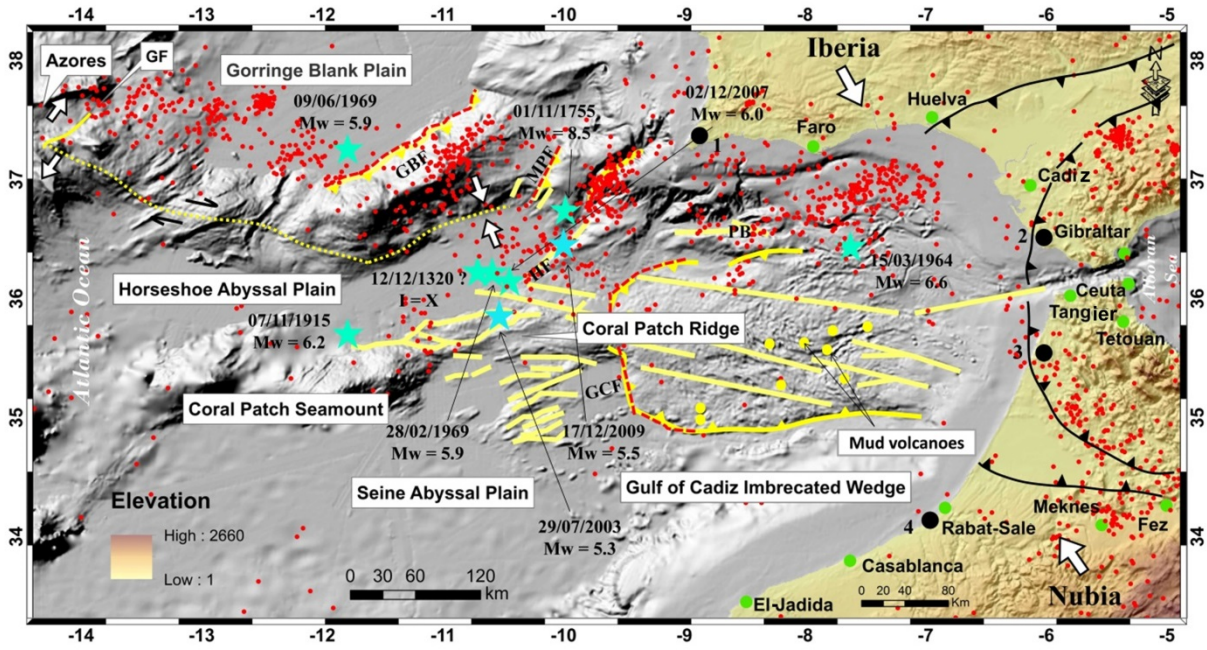

140

141 Figure 2: Bathymetry map and tectonic interpretation of the Azores-Gibraltar area modified from (Zitellini et al.,
142 2009; Bartolome et al., 2012). Earthquake epicenter distribution (red dots) from ISC Catalogue and the 1st
143 November 1755 Lisbon model earthquakes used in this study (red dashed lines). The blue stars locate the
144 epicentres of the most important events, and the black circles locate the sites where coastal mega-blocks have
145 been convincingly described (1, Furnas-Barranco; 2, Cabo of Trafalgar; 3, Larache; 4, Val d'Or). Abr: GBF,
146 Gorringe Bank Fault; MPF, Marquês do Pombal Fault; HF, Horseshoe Fault; GF, Gloria Fault; PB, Portimão
147 Bank Fault; GCF, Gulf of Cádiz Fault.

148 ## 3. Methodology

149 To evaluate tsunami hazard parameters along the studied coastline, we applied a methodology
150 illustrated by the simplified logical tree shown by Figure. 3. This approach aims to reproduce historic events
151 such as the 1755 1st November tsunami that affected the Gulf of Cadiz. To do so, the tsunami hydrodynamic
152 simulation includes three main steps: wave generation, and propagation as well as inland inundation.

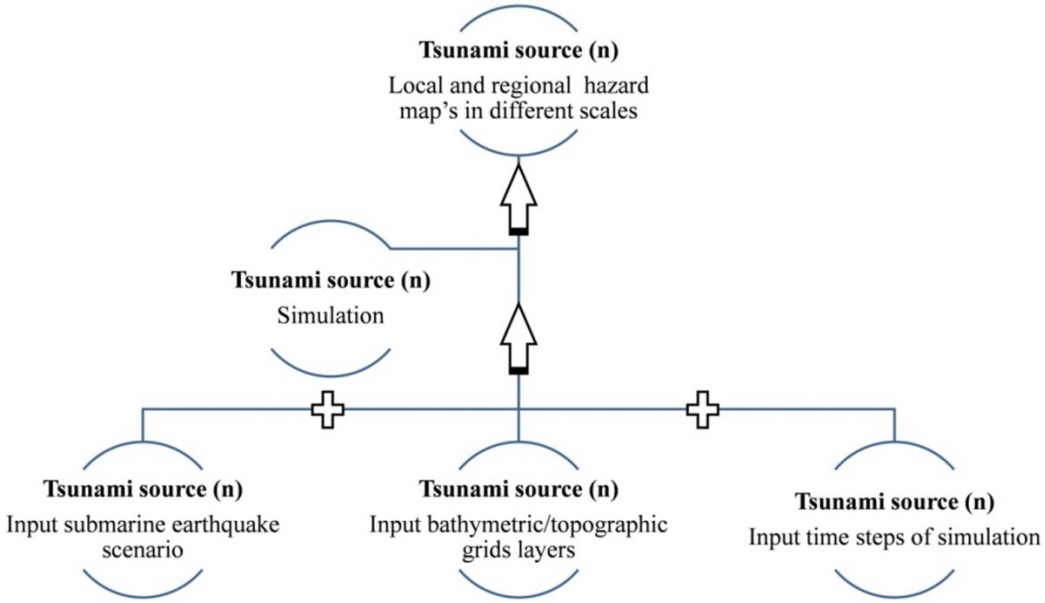

153

154 Figure 3: Logical approach to evaluate tsunami impact in study area.

155 ### 3.1. Tsunami scenarios

156 To define the seismic scenarios capable to trigger tsunamis in the Southwestern Iberian region, we
157 compiled potential tsunamigenic faults from the literature (Blanc, 2009) (Table 1 and Fig. 2) and used the focal
158 mechanisms of some selected events from the International Seismological Center (ISC, 2020) catalogue for the
159 period 1970–2007 (Mw >3).

160 We selected four earthquake scenarios that correspond to four faults in the Gulf of Cadiz (dashed red
161 lines in Fig. 2), using indicators of seismotectonic activity such as fault traces in submarine Quaternary deposits
162 and seismo-stratigraphic signatures as well as instrumental seismicity (Hayward et al., 1999; Zitellini et al.,
163 2001; Gràcia et al. 2003; Omira et al., 2009; Cunha et al., 2010; Bartolome et al., 2012; Martínez-Loriente et al.,
164 2018).

165 In these scenarios, we focused on assessment of tsunamis impact in the Gulf of Cadiz region and some
166 cities of Northern Atlantic Morocco using typical faults parameters (Table 1): Gorringe Bank, Gulf of Cadiz,
167 Marquês do Pombal, and Horseshoe faults. To model associated tsunami, the geometry of the faults was
168 simplified to a rectangle and the slip amplitude was fixed accordingly (Scholz, 1981). Therefore, the seismic

moment definition of Aki (1966) (Eq.1) and the Mo-Mw relation defined by Hanks and Kanamori, 1979 (Eq. 2) included in MIRONE software were used to compute the earthquake scenario's magnitude (Table.1).

$$M_o = \mu \times A \times D \quad (1)$$

$$\mathrm{Log}_{10}(M_o) = 1.5 \times M_w + 9.05 \quad (2)$$

where Mo is the seismic moment (Nm); A is the rupture area (km^2); μ is the crustal rigidity (Nm^{-2}), D the fault slip (m) and Mw is the moment magnitude.

Table 1: Fault parameters of the tsunamigenic scenarios used in this study. μ: the shear modulus, L: the fault length in km, W: the fault width in km, and Mw: the seismic magnitude (modified from Omira et al., 2009).

Scenarios name	**L (km)**	**W (km)**	**Epicentre coordinates (WGS84/Decimal Degrees)**		**Depth (km)**	**Slip (m)**	**Strike (◦)**	**Dip (◦)**	**Rake (◦)**	**μ (Pa)**	**Mw**
			Lon	Lat							
Gorringe Bank fault	127	60	-11.332	36.665	5.0	8.3	233.0	35	90	3.0×10^{10}	8.4
Horseshoe fault	165	70	-9.913	35.796	4.0	10.7	42.1	35	90	3.0×10^{10}	8.4
Marquês do Pombal fault	129	70	-9.890	36.574	4.0	8.0	20.0	35	90	3.0×10^{10}	8.1
Gulf of Cadiz fault	168	200	-8.059	35.407	5.0	10	349.0	5	90	3.0×10^{10}	8.6

3.2. Simulation code

Numerical simulation is an effective method to estimate the areas that will be flooded, as well as the maximum wave height and the arrival travel times of a tsunami. We used MIRONE program that allows realizing numerical simulation of the hydrodynamic process with the TINTOL code (http://fct-gmt.ualg.pt/mirone/downloads/windows.html, accessed December 2019) (Luis, 2007). To compute the

generation of a tsunami caused by an offshore seismic event, we used a linear elastic dislocation model (Mansinha and Smylie, 1971). Because this option only computes the vertical component of the deformation produced by an earthquake, it is less prone to uncertainties in the parameters and simply consists in calculating the initial vertical movement of the sea surface floor associated with a seismic rupture. As for propagation and inundation, linear (Eq.3) and non-linear (Eq.4) differential models included in MIRONE software are used, respectively (Luis, 2007).

$$\frac{\partial \eta}{\partial t} + \frac{\partial P}{\partial x} + \frac{\partial Q}{\partial y} = 0$$

$$\frac{\partial P}{\partial t} + gH + \frac{\partial \eta}{\partial x} = 0$$

$$\frac{\partial Q}{\partial t} + gH + \frac{\partial \eta}{\partial y} = 0 \qquad (3)$$

$$\frac{\partial P}{\partial t} + \frac{\partial}{\partial x}\left(\frac{P^2}{H}\right) + \frac{\partial}{\partial y}\left(\frac{PQ}{H}\right) + gH\frac{\partial \eta}{\partial x} + \tau_x = 0$$

$$\frac{\partial Q}{\partial t} + \frac{\partial}{\partial x}\left(\frac{PQ}{H}\right) + \frac{\partial}{\partial y}\left(\frac{Q^2}{H}\right) + gH\frac{\partial \eta}{\partial y} + \tau_y = 0 \qquad (4)$$

where η is the free-surface displacement, $H = \eta + h$ is the total water depth and h is the still-water depth. P and Q are the horizontal components of the volume flux in the x and y-axes, respectively, and τx and τy are the bottom friction terms in the x- and y-axes, respectively.

Finally, to propagate this initial impulsion through the oceanic water body, from the source zone to the coast, we used a series of bathymetric/topographic grids layers were downloaded from the GEBCO database (General Bathymetric Chart of the Oceans, https://www.gebco.net/data_and_products/gridded_bathymetry_data/, accessed December 2019). The time step used for tsunami simulations was 1.5 s and the computations were carried out for 3000 s. This dataset was nested in a grid system with different resolutions for consecutive calculations of tsunami event generation, propagation in an open boundary condition and inland inundation. The main grid layer has a 300 m-resolution and is used for tsunami propagation in the Gulf of Cadiz. The second grid layers, improved by transplanting the main grid layer of 300 m using 'transplant 2nd grid tool' (Luis, 2007), have a high resolution (60 m, 15 m, 10 m and 2 m) and are used for the inland inundation of selected cities exposed to tsunami along the Atlantic coast of Morocco (El-Jadida, Casablanca and Mohammedia).

4. Results

For each earthquake scenario, tsunami simulation was produced to derive the following parameters: spatial and temporal distribution of Maximum Water Elevation (MWE), Maximum Inundation Distance (MID), and Maximum Flow Depths (MFD). The MWE shows the large-scale tsunami energy direction toward the coasts around the Gulf of Cadiz, whereas the MFD, and MID were computed to evaluate the local impact of simulated tsunamis in selected areas along the Northern Atlantic coast of Morocco.

4.1. Maximum Water Elevation and tsunami arrival travel time estimate

For the four earthquake scenarios, the results of MWE calculations are presented in Figures 4, 5, 6 and 7 respectively, with the results of arrival travel time, from the epicenter source to the coast that locates the highest tsunami waves. In our simulations, all earthquake scenarios steered tsunami energy towards the Gulf of Cadiz region including the south-western coasts of the Iberian Peninsula and the Northern Atlantic coasts of Morocco. However, there are differences in the main direction of maximum energy as well as in the time required to reach the coastal regions.

The scenario involving Cadiz Wedge in front of the Gulf of Cadiz Fault (Mw = 8.6: Table. 1) has been considered as a possible source of the 1755 event (*e.g.*, Gutscher, 2004). In figure 4-a, the simulation indicates that the wave front generated by this scenario is directed towards the coasts of all cities around the Gulf of Cadiz, with a greater MWE in south-western Iberian Peninsula than along the Northern Atlantic coasts of Morocco. In this scenario, the tsunami impact would significantly affect coastline between Larache and El-Jadida. In the offshore area, the tsunami waves have equal amplitudes. Nevertheless, change in bathymetry affects the wave speed, which can abruptly produce a MWE reaching up to 6 m in some locations (Fig. 4-a). The estimation of the arrival travel time for the tsunami waves is on the order of 65 min along the Northern coasts of Morocco (Fig. 4-b).

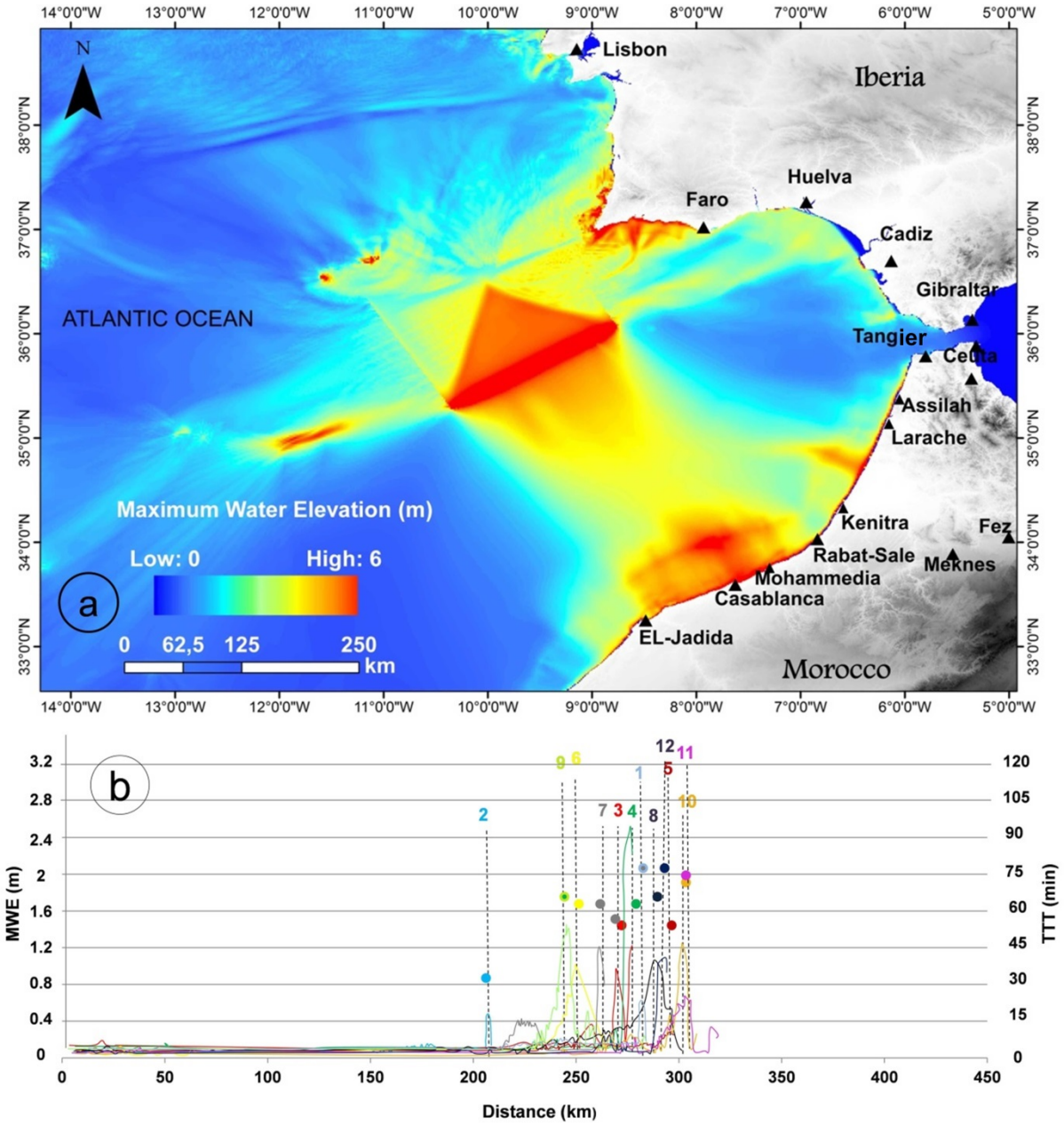

230

231 Figure 4: Results of the propagation for the Gulf of Cádiz Fault in south-western coasts of Iberian Peninsula and
232 Northern of Morocco coasts, (a) wave height from the epicentre zone to the coast and (b) tsunami arrival travel
233 times (TTT) at selected cities (1, Lisbon; 2, Faro; 3, Huelva; 4, Cadiz; 5, Tangier; 6, Assilah; 7, Larache; 8,
234 Kenitra; 9, Rabat-Sale; 10, Mohammedia; 11, Casablanca; 12, El-Jadida)

235 The Marquês do Pombal Fault is located in the active tectonic region between the Gorringe Bank and the Coral
236 Patch Ridge zone (Fig. 2) (Johnston, 1996; Zitellini et al., 2001). With a M_w of 8.1 (Table 1), the tsunami may
237 cause severe destructions to coastal cities of Morocco, Portugal, and Spain. In figure 5-a, the simulation displays

238 that the wave front generated by this scenario would be directed towards the coasts of Larache, Casablanca,
239 Rabat-Sale, El-Jadida, Cadiz, Faro and Lisbon. MWE computations for Marquês do Pombal Fault along of the
240 coasts exposed to this scenario may reach up to 24 m in some areas (Fig.5-a). Examination of these results
241 indicates that the tsunami impact in some locations is low (*i.e.,* Northern of Kenitra) because of the local
242 bathymetry. Moreover, the estimated magnitude of 8.1 (Table. 1) is less than for other faults considered in this
243 study. Therefore, MWE results show sites where the tsunami energy is weaker (Kenitra and surrounding coasts)
244 than in others. The arrival travel time estimation could be about 95 min along the Northern coasts of Morocco
245 because of the long distance traveled (Fig. 5-b).

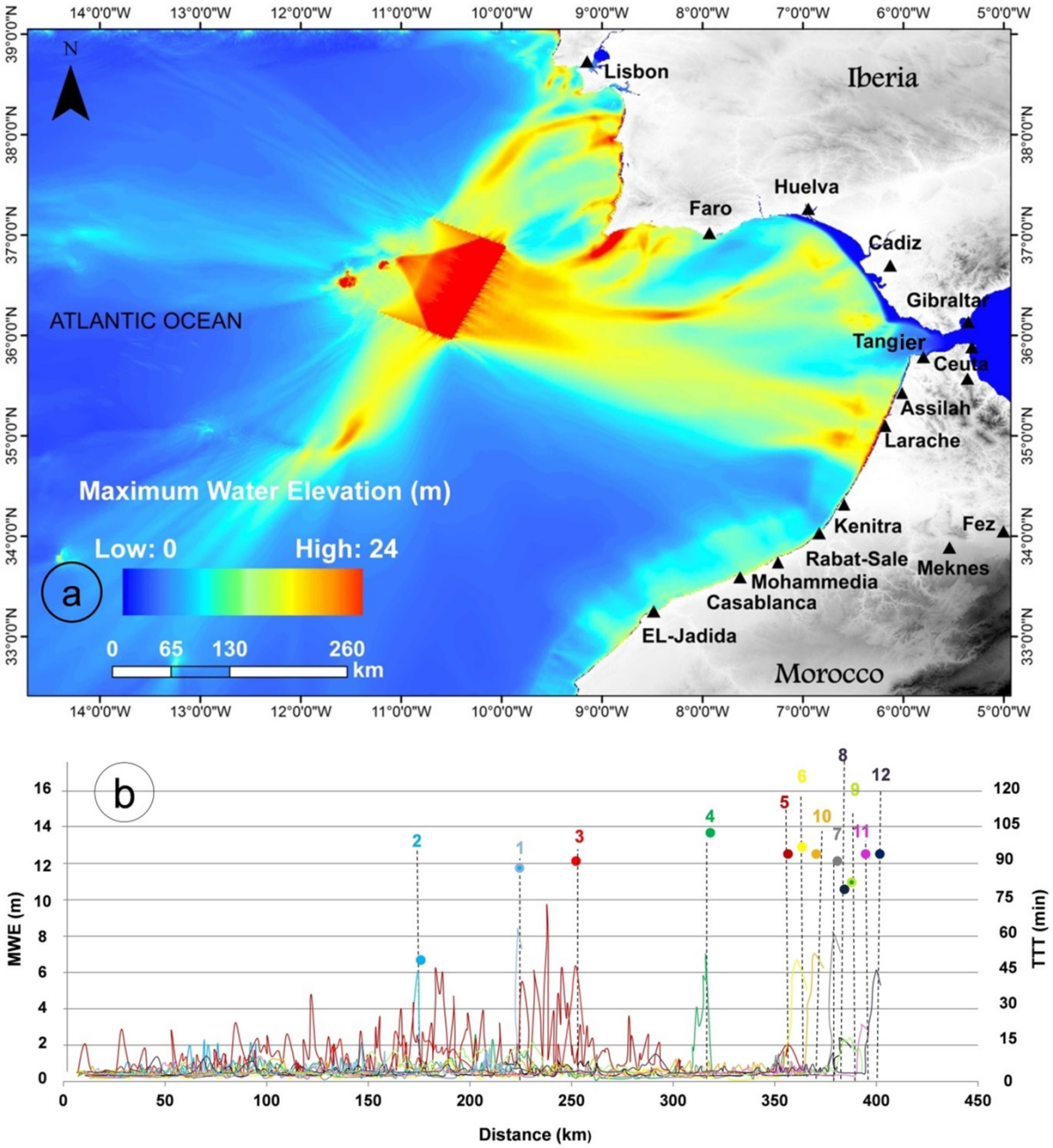

246

247 Figure 5: Results of the propagation for the Marquês do Pombal Fault in south-western coasts of Iberian
248 Peninsula and Northern of Morocco coasts, (a) wave height from the epicentre zone to the coast and (b) tsunami
249 arrival travel times (TTT) at selected cities (1, Lisbon; 2, Faro; 3, Huelva; 4, Cadiz; 5, Tangier; 6, Assilah; 7,
250 Larache; 8, Kenitra; 9, Rabat-Sale; 10, Mohammedia; 11, Casablanca; 12, El-Jadida)

251 The Gorringe Bank Fault may be the source for the 1755 earthquake because of its associated active uplift and
252 shortening (*e.g.,* Johnston, 1996). In figure 6-a, the simulation displays tsunami waves that are directed towards
253 three different directions in the Gulf of Cadiz. Part of the waves created is directed towards the Portuguese coast,

with a MWE ranging from 2 to 8 m at Faro and reach up to 20 m in the south of Lisbon (Fig. 6-a). Another part is directed towards the Gibraltar Strait and is characterized by MWE lower than 6 m at Cadiz (Fig. 6-a). The last part is directed towards the Moroccan coasts and is characterized by very high amplitudes up to 10 m close to Casablanca and surrounding areas (Fig. 6-a). The estimated arrival travel time could be about 99 min along the studied coastal area (Fig. 6-b).

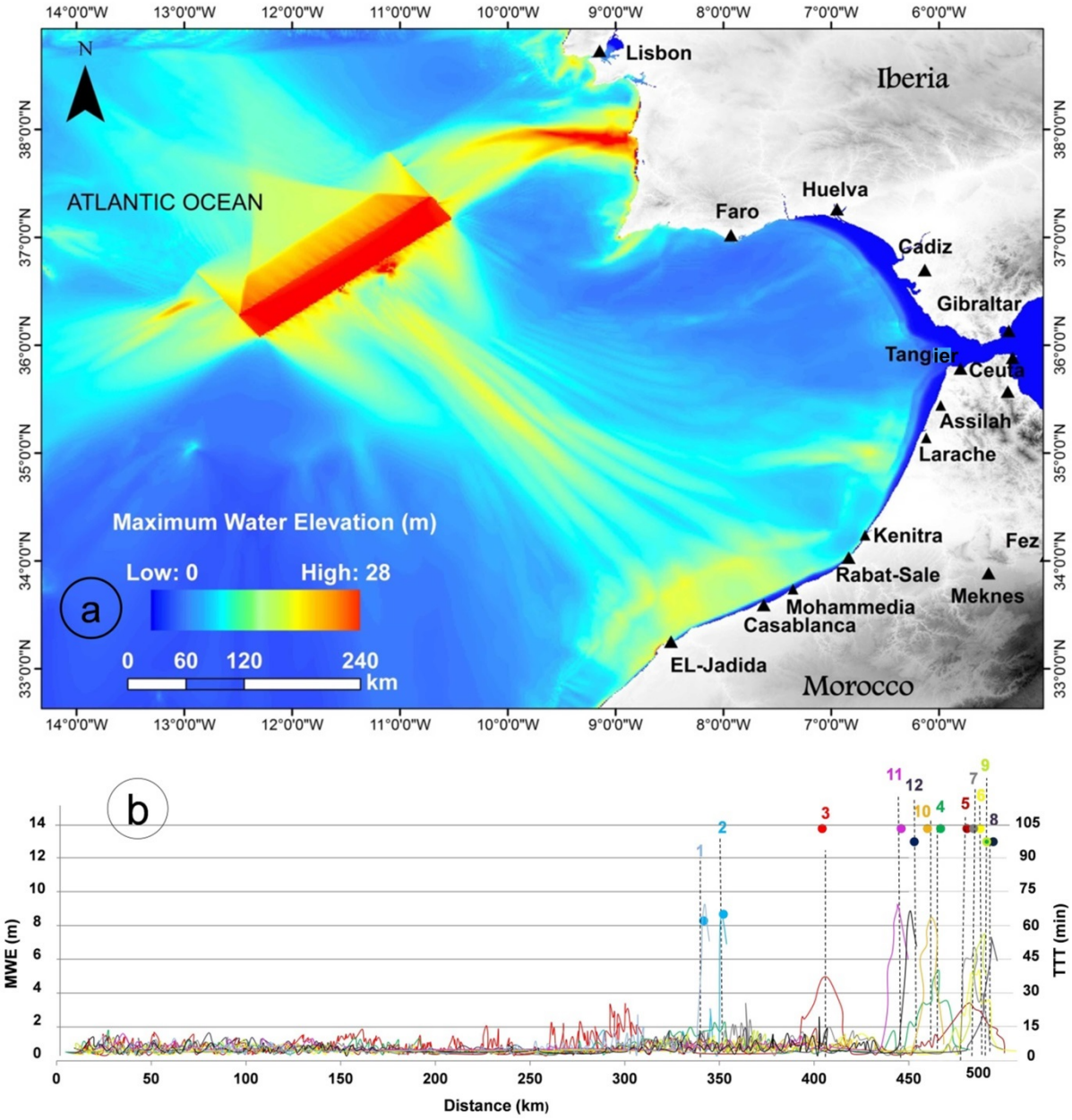

Figure 6: Results of the propagation for the Gorringe Bank Fault in south-western coasts of Iberian Peninsula and Northern of Morocco coasts, (a) wave height from the epicentre zone to the coast and (b) tsunami arrival

travel times (TTT) at selected cities (1, Lisbon; 2, Faro; 3, Huelva; 4, Cadiz; 5, Tangier; 6, Assilah; 7, Larache; 8, Kenitra; 9, Rabat-Sale; 10, Mohammedia; 11, Casablanca; 12, El-Jadida)

In figure 7-a, we present the results of MWE and tsunami wave's directions for the Horseshoe Fault scenario. First, this potential earthquake has an epicenter zone very close to the others and has almost the same orientation, except to that of Gulf of Cadiz Fault. Whereas the magnitude of this earthquake scenario is like that of Gorringe Bank Fault, it would create higher waves and larger tsunami energy over the coastal zones of Morocco. The principal directions of tsunami energy are to the South (El-Jadida), to South-Southeast (Mohammedia-Casablanca-Kenitra-Rabat), to the Southeast (Larache-Tangier-Assilah-Gibraltar), to the East (Cadiz), and to the Northeast (Huelva-Faro). Within this scenario, the MWE may reach up to 10 m, 23 m, 25 m, 10 m and 10-25 m according to these directions, respectively (Fig. 7-a). The tsunami may significantly affect the coastlines of Casablanca, Mohammedia and Larache. During the simulation, the tsunami waves spread out and reached the Northern Atlantic coasts of Morocco in a shorter time (~79 min), unlike the other scenarios (Gorringe Bank and Marquês do Pombal faults) (Fig. 7-b). The result of MWE computations reach about 23 m for Horseshoe Fault along most of the coasts exposed to this scenario, with a maximum energy towards Mohammedia and Larache coastal areas (Fig. 7-a). Consequently, the tsunami wave near the Moroccan coastline, and the energy generated by the Horseshoe Fault could be very high. These results suggest that this scenario is the worst tsunami case for the Moroccan coasts, as well as in some other areas along the coastal areas of the south-western of Iberian Peninsula.

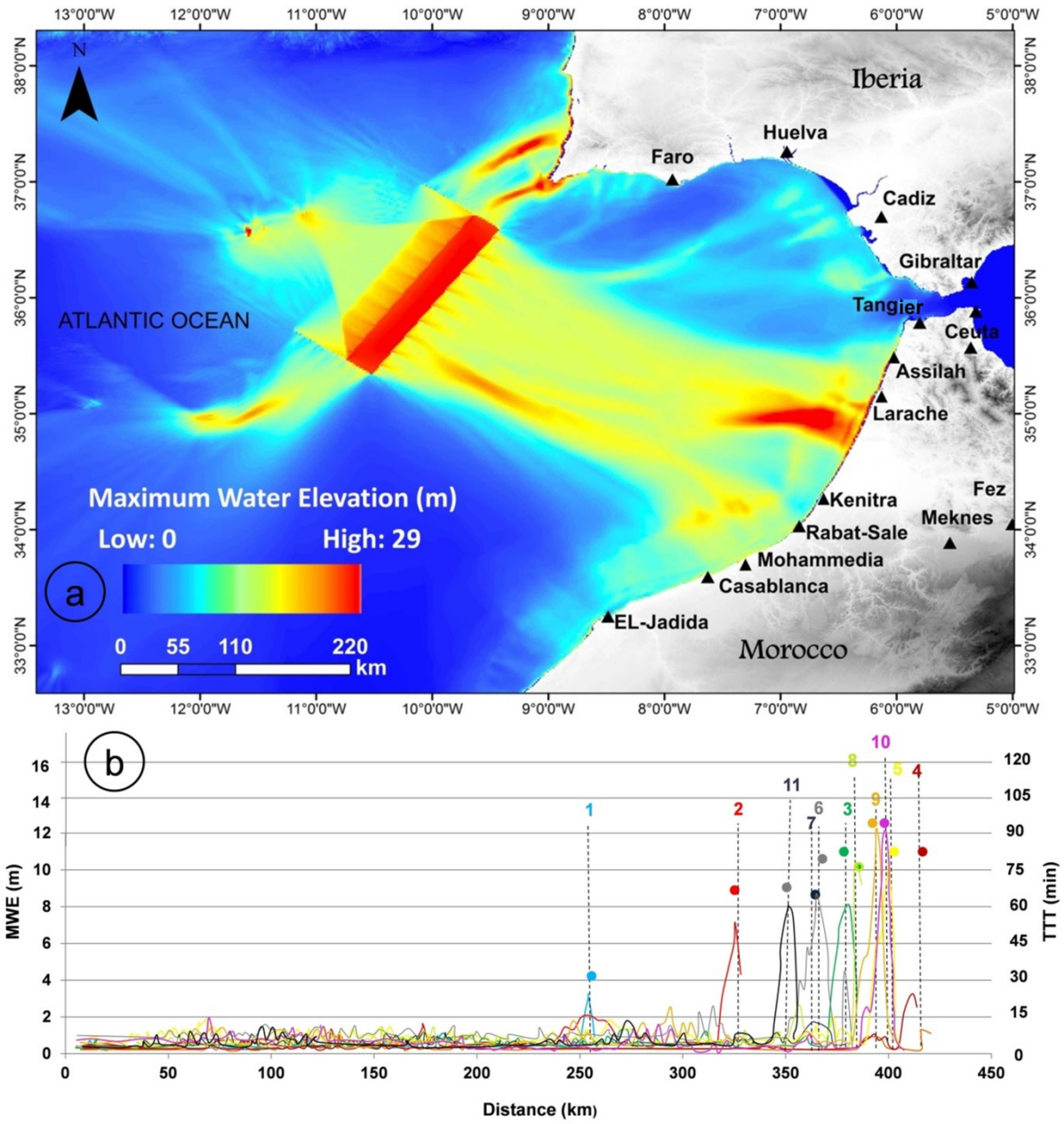

280

281 Figure 7: Results of the propagation for the Horseshoe Fault in south-western coasts of Iberian Peninsula and
282 Northern of Morocco coasts, (a) wave height from the epicentre zone to the coast and (b) tsunami arrival travel
283 times (TTT) at selected cities (1, Faro; 2, Huelva; 3, Cadiz; 4, Tangier; 5, Assilah; 6, Larache; 7, Kenitra; 8,
284 Rabat-Sale; 0, Mohammedia; 10, Casablanca; 11, El-Jadida)

285 **4.2. Impact and Mapping Inundation**

286 The results of MID, MFD, and MIA computations and spatial distribution with arrival travel times on
287 the exposed cities along the Northern Atlantic coasts of Morocco for the worst scenario associated to Horseshoe

Fault are presented in figures 8 and 9, which display the results for the considered cities (El-Jadida, Casablanca, and Mohammedia). Figure 8-a shows the tsunami impact at El-Jadida. In this city, the MFD ranges from 5 to 6 m and the MID reaches 2.2 km and 2 km in the surrounding areas of the hypodrome and harbor, respectively (Fig.8-b). We also present the tsunami impact generated by the Horseshoe Fault scenario at Casablanca, which produces a MFD ranging from 8 m to 10 m (Fig.8-c) and a MID of about 2.8 km at the harbor (Fig.8-d). This scenario produces height impact along the coast of Mohammedia city, with the MFD ranging from 8 m to 10 m (Fig.8-e). The MID reaches 4.6 km at the location of the oil refinery “La Samir” and surrounding areas (city beach, and oil harbor) because of the flat topography and rivers (Dir and Mellah), where the inundation extends even more, flooding large land surfaces (Fig.8-f).

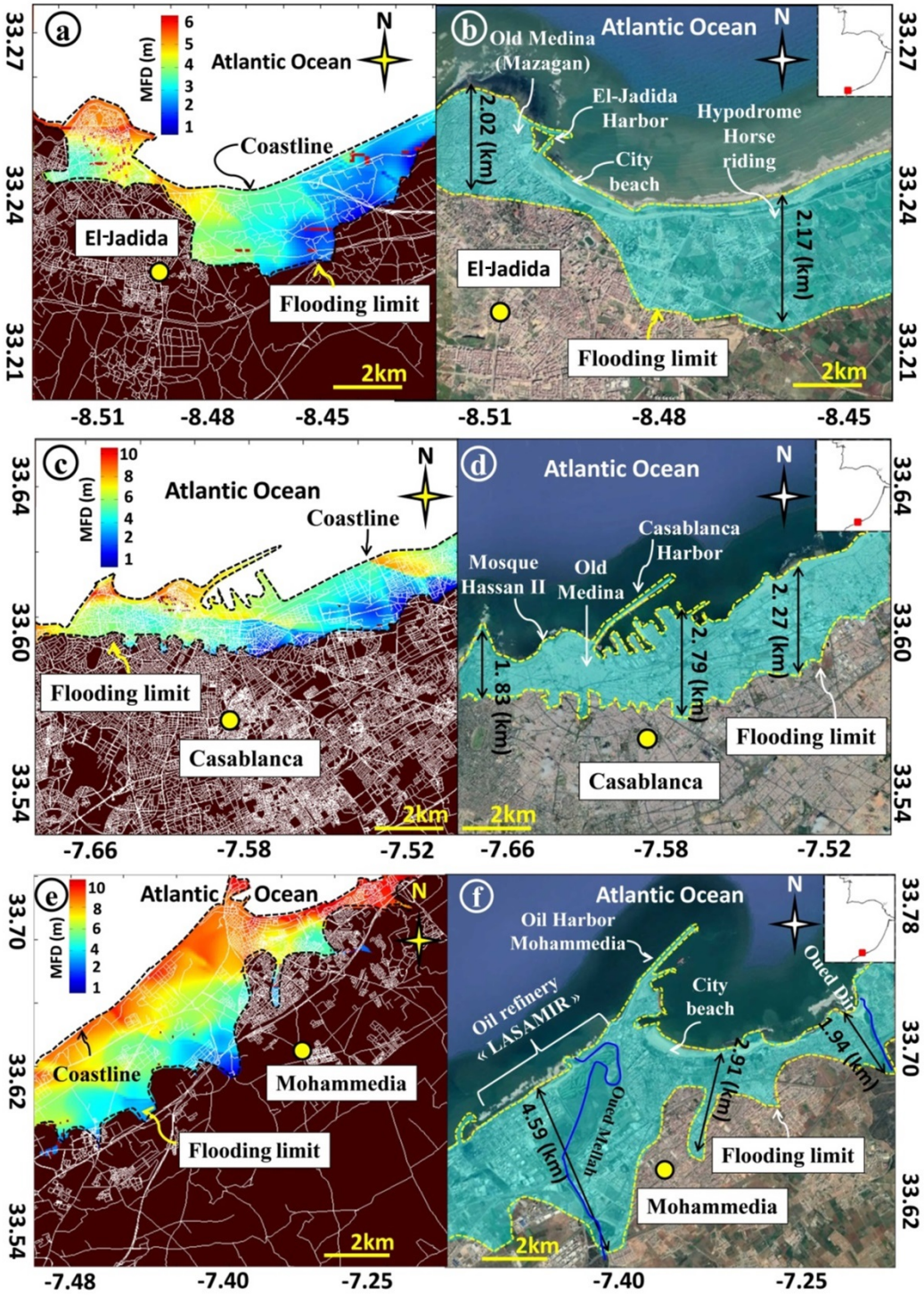

297

298 Figure 8: Flooding maps and computed inundation distances for the Horseshoe Fault scenario on the selected
299 exposed cities along the Northern Atlantic coast of Morocco: (a) MFD and (b) MID at El-Jadida; (c) MFD and
300 (d) MID at Casablanca; (e) MFD and (f) MID at Mohammedia.

301

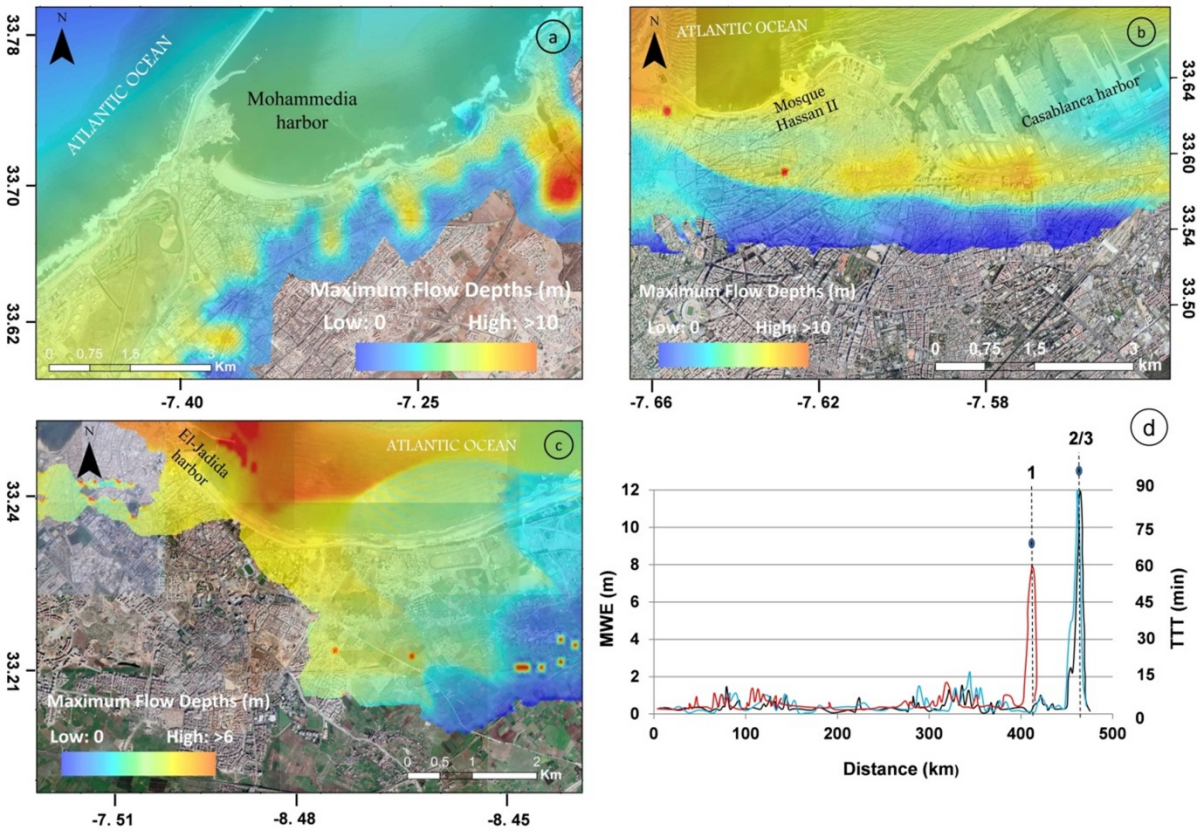

Figure 9: Results inundated area and maximum flow depths, for the Horseshoe Fault scenario along the harbors and principal locations in (a) Mohammedia, (b) Casablanca, (c) El-Jadida with high resolution inundation maps 2 m, 10 m and 15 m respectively and (d) maximum tsunami water elevation (MWE) along the coastline and tsunami arrival travel times (TTT) at selected locations (1- El-Jadida and 2/3- Casablanca & Mohammedia).

5. Discussion

5.1. Comparison with other model results and historical data

The simulation maps show that maximum flow depth generated by the Horseshoe Fault scenario, which we assumed to be the scenario triggering the worst tsunami impact on considered coastal cities and surrounding areas. The harbors of these cities are completely flooded, the inundation depth reaching 6 m at El-Jadida and 10 m at both Casablanca and Mohammedia. Moreover, the maximum area flooded located at Mohammedia harbor (the main oil port of Morocco) and in "La Samir" refinery. This site constitutes an important issue as it comprises not only the refinery but also the largest thermal electric central in the country, which largely supplies the region of Casablanca.

The maximum flow depth decreases progressively from the coastline towards the inundation boundary because of the variation of topography and energy dissipation. Furthermore, simulation results are influenced by

the fault strike (Satake et al., 2007) and the basin bathymetry that constrains the tsunami energy distribution (Omira et al., 2011). The maximal tsunami amplitude is perpendicular to the fault strike (Titov, 1999), and the decrease in bathymetry amplifies the wave amplitude along the coasts. Therefore, the characteristic parameters (strike, dip and slip) of candidate tsunamigenic sources may affect the MWE and the rake or slip angle on the fault plane, which also plays an important role on the initial deformation. On the other hand, the results of three earthquake scenarios associated with the Horseshoe, Marquês do Pombal, and Gorringe Bank faults show some degrees of compatibility with both historical tsunami impact observations and description of geomorphic and sedimentary deposits in Spain (Whelan and Kelletat, 2005), Portugal (Scheffers and Kelletat, 2005) and along the Northern coast of Morocco (Medina et al., 2011; El Talibi et al., 2016, 2021). If the Horseshoe Fault, with some differences in the maximum level of waves heights due to the limitation of MIRONE software (see section 5.2), appears to be the more impacting potential source, in agreement with previous models (Omira et al., 2009, 2010 ; Lima et al., 2010; Mellas et al., 2012; Benchekroun et al., 2015 and El Moussaoui et al., 2017), the analysis of tsunami propagation close to the shoreline indicate that waves have similar behavior for the three scenarios, most probably because of the proximity of the sources as well as their similar orientations. If Assilah and Larache are at equal distance (360 km) from the epicenter of Marquês do Pombal and Horseshoe faults, the difference in waves arrival travel time after earthquake that reach to 95 and 80 respectively (difference of 15 min), reflects the propagation velocity of the two wave trains consequently to bathymetry variations and differences in energies released towards the Moroccan coasts (see Fig. 5-b and Fig. 7-b). According to our simulation, the MWE in El-Jadida should be less than 10 m, which disagrees with historical records (*e.g.,* Soyris, 1755). However, Blanc (2009) estimated that the MWE of the 1755 tsunami, reported along the shoreline of Morocco between Agadir and Tangier, was 2.5 m. Indeed, our results show that the worst energy of Horseshoe scenario is steered between Tangier and El-Jadida coasts. This is in agreement with the historical data that indicate that the tsunami impact was greater in Northern Atlantic coasts of Morocco than along the southern coasts (Kaabouben et al., 2009). However, these authors show that at El-Jadida city, the flooding limit reaches roughly 0.7 km, which is smaller than the 2 km inland calculated in this work. Nevertheless, according to the tsunami travel time calculated using the ray tracing technique by Omira et al. (2009), as well as to evacuation model used in Tadibaght et al. (2022), the Northern Atlantic population of Morocco can safely evacuate if the tsunami event were to occur in daytime and the evacuation were to start 1 hour after the triggering of tsunami waves or earlier.

5.2. Validity and limitations of tsunami simulation

Despite the improvement of the bathymetric/topographic data in the MIRONE software, the 300 m resolution (www.Gebco.net) is a limitation especially in hazard mapping at the local scale. Thus, the results obtained in this work may be influenced by protective structures in ports and by submarine canyons. The latter cannot be detected due to the low resolution of the input data, but may change the amplitude of wave breaking and the tsunami energy. However, according to Wynn et al. (2000), maps of submarine canyons in Morocco show that they exist only in the south of El-Jadida. So, the effect of these canyons can be regarded as negligible.

We restricted the scenarios to four major faults (Gorringe Bank, Marquês do Pombal, Horseshoe, Gulf of Cádiz), considering that they are active and responsible for recent seismic events in the Gulf of Cadiz (*e.g.,* Zitellini et al., 2001; Silva et al., 2017). The magnitude calculated for each scenario by MIRONE software can be influenced by the geometry of the source area and by the number of fault segments such as the complex seismic scenarios proposed by Fonseca, (2020), which also considers the accretionary prism as a potential source for seismic events in the Gulf of Cadiz. However, MIRONE software (Open-source tool) gives good results comparable with commercial software of more limited access (*e.g.,* Omira et al. 2012). Moreover, MIRONE is one of the most popular programs in the scientific community due to its high quality of cartography and graphing capabilities (Luis, 2007).

According to other results in the three scenarios Gorringe Bank, Marquês do Pombal and Horseshoe faults, the MWE higher than 10 meters and the distance inundation reach up to 1 km are overestimated and unrealistic values (*e.g.,* Mellas et al. 2012; Omira et al. 2012; Omira et al. 2015). But, an event of such magnitude is still possible, since in Morocco there are cities like Mazagan (El-Jadida) that were affected by the 1755 event despite their geographical location exceeding 10 meters (*e.g.,* Soyris, 1755; El Mrabet, 2005).

6. Conclusion

In this paper, we simulated scenarios of tsunami flooding in some cities along the Northern Atlantic coasts of Morocco for the earthquake sources located in the offshore of the Gulf of Cadiz region. To do this, we used the parameters of scenario sources by the integration in MIRONE numerical code combining a series of bathymetric /topographic grid layers with an initial water elevation (sea-surface perturbation) generated using Mansinha's formulations and assuming an instantaneous seabed displacement. Using MIRONE software (Open-source tool), results indicate that the Horseshoe Fault is the worst scenario, which produced the largest tsunami toward the Northern Atlantic coasts of Morocco. Through our literature review and results, we can say that it is the most likely source of a potential tsunami. This scenario computed a MWE that may exceed 20 m in some area, the MFD and MID range respectively from 8 m to 10 m and 1.9 km to 4.6 km inland at "La Samir" in

Mohammedia. Moreover, the computed MWE ≤ 10 m at EL-Jadida show a large disagreement with historical reports in some locations and agreement with numerical model results. Tsunami impact calculated at both Casablanca and Mohammedia is the same except the inland distance that is less at Casablanca. However, the economic and touristic areas are exposed to west-Iberian tsunamis in the Northern of Morocco. Therefore, economic and social impacts of a major tsunami along these coasts may have large consequences, either directly: power generating units and power and gas supply at Mohammedia; losses for industry, shipping and navigation, especially at Casablanca; loss of agricultural production by loss of crops and contamination of soils, especially at El-Jadida and surrounding areas, or indirectly: destruction of hospital and medical centre buildings and equipments, emergence of water vector-borne diseases following sea water inundation of freshwater bodies. On this basis and in absence of early warning system, risk education of coastal communities is one of the main preventive actions in the case of a future event.

Highlights

- Characteristics of potential tsunami sources around the Gulf of Cadiz.
- Simulation the impacts of tsunami on some cities along the Northern Atlantic coasts of Morocco.
- MIRONE software as reliable open-source tool for tsunami waves simulation.

Acknowledgment

This work is part of the RiskMED project, Labex OT-Med (ANR–11–LABE–0061), supported by the Investissements d'Avenir, French Government project of the French National Research Agency (ANR) through the A*Midex project (ANR–1—IE–0001–02). The authors thank all reviewers for the constructive and valuable comments.

Declaration of competing Interest

The authors declare having no conflict of interest.

References

Aki, K.., 1966. Generation and Propagation of G Waves from the Niigata Earthquake of June 16, 1964. Bull. Earthq. Res. Inst. 44

Andrade, C., 1992. Tsunami generated forms in the Algarve barrier islands (South Portugal). Sci. Tsunami Haz. 10, 21–34.

Baptista, M.A., Miranda, P., Victor, L.M., 1992. Maximum entropy analysis of Portuguese tsunami data; the tsunamis of 28.02. 1969 and 26.05. 1975. Sci. Tsunami Hazards 10, 9–20.

Baptista, M.A., Miranda, P.M.A., Miranda, J.M., Victor, L.M., 1998. Constrains on the source of the 1755 Lisbon tsunami inferred from numerical modelling of historical data on the source of the 1755 Lisbon tsunami. J. Geodyn. 25, 159–174.

Baptista, M. A., Miranda, J. M., Batlló, J., Lisboa, F., Luis, J., & Maciá, R., 2016. New study on the 1941 Gloria Fault earthquake and tsunami. Natural Hazards and Earth System Sciences, 16(8), 1967-1977.

Baptista, M. A., 2020. Tsunamis along the Azores Gibraltar plate boundary. Pure and Applied Geophysics, 177(4), 1713-1724.

Barkan, R., Uri, S., & Lin, J., 2009. Far field tsunami simulations of the 1755 Lisbon earthquake: Implications for tsunami hazard to the US East Coast and the Caribbean. Marine Geology, 264(1-2), 109-122.

Bartolome, R., Gràcia, E., Stich, D., Martinez-Loriente, S., Klaeschen, D., de Lis Mancilla, F., Lo Iacono, C., Dañobeitia, J.J., Zitellini, N., 2012. Evidence for active strike-slip faulting along the Eurasia-Africa convergence zone: Implications for seismic hazard in the southwest Iberian margin. Geology 40, 495–498.

Benchekroun, S., Omira, R., Baptista, M.A., El Mouraouah, A., Brahim, A.I., Toto, E.A., 2015. Tsunami impact and vulnerability in the harbour area of Tangier, Morocco. Geomatics, Nat. Hazards Risk 6, 718–740.

Blanc, P.-L., 2008. The tsunami in Cadiz on 1 November 1755: A critical analysis of reports by Antonio de Ulloa and by Louis Godin. Comptes Rendus Geosci. 340, 251–261.

Blanc, P.-L., 2009. Earthquakes and tsunami in November 1755 in Morocco: a different reading of contemporaneous documentary sources. Nat. Hazards Earth Syst. Sci. 9, 725–738.

Buforn, E., Udias, A., Mezcua, J., 1988. Seismicity and focal mechanisms in south Spain. Bull. Seismol. Soc. Am. 78, 2008–2024.

Buforn E., Bezzegoud M., Udias A., Pro C., 2004. Seismic sources on the Iberia-African plate boundary and their tectonic implications. Pure Appl Geophys 161:623–626

Chadha, R.K., Latha, G., Yeh, H., Peterson, C., Katada, T., 2005. The tsunami of the great Sumatra earthquake of M 9.0 on 26 December 2004--Impact on the east coast of India. Curr. Sci. 1297–1301.

Cunha PP, Buylaert JP, Murray AS, Andrade C, Freitas MC, Fatela F, Munhá JM, Martins AA, Sugisaki S., 2010. Optical dating of clastic deposits generated by an extreme marine coastal flood: The 1755 tsunami deposits in the Algarve (Portugal). Quat Geochronol 5:. https://doi.org/10.1016/j.quageo.2009.09.004

Dabrio, C.J., Goy Goy, J.L., Zazo Cardeña, C., 1998. The record of the tsunami produced by the 1755 Lisbon earthquake in Valdelagrana spit (Gulf of Cádiz, southern Spain). Geogaceta 23, 31–34.

DAT (Direction de l'Aménagement du Territoire)., 2017. Élaboration de la stratégie nationale de gestion intégrée du littoral - Phase 2 : Diagnostic stratégique du littoral. https://www.muat.gov.ma/sites/default/files/Documentation/17.pdf. Accessed 6 Oct 2021

Dill, H.G. and Kaufhold, S., 2018. The Totumo mud volcano and its near-shore marine sedimentological setting (North Colombia) – From sedimentary volcanism to epithermal mineralization.- Sedimentary Geology 366: 14-31.

Dill H.G., Buzatu A., Goldmann S., Kaufhold S., and Bîrgăoanu d., 2020. Coastal landforms of "Meso-Afro-American" and "Neo-American" landscapes in the periglacial South Atlantic Ocean: With special reference to the clast orientation, morphology, and granulometry of continental and marine sediments. Journal of South American Earth Sciences 98: 102385

Dill, H.G., 2022. Trends and composition – A sedimentological-chemical-mineralogical approach to constrain the origin of Quaternary deposits and landforms - From the review to the manual.- Geosciences: 1497156 , 59 pp.

El Moussaoui, S., Omira, R., Zaghloul, M.N., El Talibi, H., Aboumaria, K., 2017. Tsunami hazard and buildings vulnerability along the Northern Atlantic coast of Morocco--the 1755-like tsunami in Asilah test-site. Geoenvironmental Disasters 4, 1–14.

El Mrabet, T., 2005. The great earthquakes in the Maghreb region and their consequences on man and environment. CNRS-LAG report, Rabat, Morocco (in Arabic). ISBN-9954-0-3777-2

El Mrini, A. (2011). Evolution morphodynamique et impact des aménagements sur le littoral tétouanais entre Ras Mazari et Fnideq (Maroc nord occidental). PhD Thesis, France: Université Abdelmalek Essaadi, Morocco and Université de Nantes, 303p.

El Talibi H El, Moussaoui S El, Zaghloul MN, Aboumaria K, Wassmer P, Mercier JL., 2016. New sedimentary and geomorphic evidence of tsunami flooding related to an older events along the Tangier-Asilah coastal plain, Morocco. Geoenvironmental Disasters 3:. https://doi.org/10.1186/s40677-016-0049-6

El Talibi, H., El Moussaoui, S., Aboumaria, K., Wassmer, P., Mercier, J.L., 2021. Geological evidence of high-energy marine flooding events on the Tangier coastal plain, Morocco. Euro-Mediterranean J. Environ. Integr. 6, 1–18.

Fonseca, J.F.B.D., 2020. A Reassessment of the Magnitude of the 1755 Lisbon Earthquake A Reassessment of the Magnitude of the 1755 Lisbon Earthquake. Bulletin of the Seismological Society of America 110 (1): 1–17. https://doi.org/10.1785/0120190198

Gjevik, B., Pedersen, G., Dybesland, E., Harbitz, C. B., Miranda, P. M. A., Baptista, M. A., & Guesmia, M., 1997. Modeling tsunamis from earthquake sources near Gorringe Bank southwest of Portugal. Journal of Geophysical Research: Oceans, 102(C13), 27931-27949.

Goff, J.R., Lane, E., Arnold, J., 2009. The tsunami geomorphology of coastal dunes. Nat. Hazards Earth Syst. Sci. 9, 847–854.

Goff, J., Chagué-Goff, C., Nichol, S., Jaffe, B., Dominey-Howes, D., 2012. Progress in palaeotsunami research. Sediment. Geol. 243, 70–88.

Goto, K., Ikehara, K., Goff, J., Chagué-Goff, C., & Jaffe, B., 2014. The 2011 Tohoku-oki tsunami—Three years on. Marine Geology, 358, 2-11.

Gràcia E, Danobeitia J, Vergés J, Bartolomé R, Córdoba D., 2003. Crustal architecture and tectonic evolution of the Gulf of Cadiz (SW Iberian margin) at the convergence of the Eurasian and African plates. Tectonics 22:. https://doi.org/10.1029/2001tc901045

Grandin, R., Borges, J.F., Bezzeghoud, M., Caldeira, B., Carrilho, F., 2007. Simulations of strong ground motion in SW Iberia for the 1969 February 28 (M s= 8.0) and the 1755 November 1 (M~ 8.5) earthquakes--I. Velocity model. Geophys. J. Int. 171, 1144–1161.

Gutscher, M. A., Malod, J., Rehault, J. P., Contrucci, I., Klingelhoefer, F., Mendes-Victor, L., & Spakman, W.., 2002. Evidence for active subduction beneath Gibraltar. Geology, 30(12), 1071-1074.

Gutscher, M.-A., 2004. What caused the great Lisbon earthquake? Science 305:1247–1248. https://doi.org/10.1126/science.1101351

Gutscher, M.-A., Baptista, M.A., Miranda, J.M., 2006. The Gibraltar Arc seismogenic zone (part 2): constraints on a shallow east dipping fault plane source for the 1755 Lisbon earthquake provided by tsunami modeling and seismic intensity. Tectonophysics 426, 153–166.

Hall, A.M., Hansom, J.D., Jarvis, J., 2008. Patterns and rates of erosion produced by high energy wave processes on hard rock headlands: The Grind of the Navir, Shetland, Scotland. Mar. Geol. 248, 28–46.

Hanks, T.C., Kanamori, H., 1979. A moment magnitude scale. J. Geophys. Res. Solid Earth 84, 2348–2350.

Hayward, N., Watts, A.B., Westbrook, G.K., Collier, J.S., 1999. A seismic reflection and GLORIA study of compressional deformation in the Gorringe Bank region, eastern North Atlantic. Geophys. J. Int. 138, 831–850.

HCP (Haut Commicariat au Plan)., 2014. Recensement général de la population humaine. http://rgphentableaux.hcp.ma/Default1/. Accessed 6 Apr 2021

Heinrich Ph, Baptista MA, Miranda P., 1994. Numerical simulation of the 1969 tsunami along the Portuguese coast. Preliminary results. Sci Tsunami Hazard 12(1):3–23

Hoffmann, G., Reicherter, K., Wiatr, T., Grützner, C., Rausch, T., 2013. Block and boulder accumulations along the coastline between Fins and Sur (Sultanate of Oman): tsunamigenic remains? Nat. hazards 65, 851–873.

ISC (International Seismological Centre., 2020. On-line Bulletin. https://earthquake.usgs.gov/earthquakes/search/. Accessed 11 Dec 2020

Jing, H.H., Zhang, H., Yuen, D.A., Shi, Y., 2013. A revised evaluation of tsunami hazards along the Chinese coast in view of the Tohoku-Oki Earthquake. Pure Appl. Geophys. 170, 129–138.

Johnston, A.C., 1996. Seismic moment assessment of earthquakes in stable continental regions. III. New Madrid 1811--1812, Charleston 1886 and Lisbon 1755. Geophys. J. Int. 126, 314–344.

Kaabouben, F., Baptista, M.A., Iben Brahim, A., Mouraouah, A. El, Toto, A., 2009. On the moroccan tsunami catalogue. Nat. Hazards Earth Syst. Sci. 9, 1227–1236.

Laouina, A., 2019. Note de recherche--Le littoral dans le développement du Maroc et de sa politique atlantique. Norois 41–54.

Levret, A., 1991. The effects of the November 1, 1755 Lisbon earthquake in Morocco. Tectonophysics 193, 83–94.

Lima, V. V, Miranda, J.M., Baptista, M.A., Catalão, J., Gonzalez, M., Otero, L., Olabarrieta, M., Álvarez-Gómez, J.A., Carreño, E., 2010. Impact of a 1755-like tsunami in Huelva, Spain. Nat. Hazards Earth Syst. Sci. 10, 139–148.

Luis, J.F., 2007. Mirone: A multi-purpose tool for exploring grid data. Comput. \& Geosci. 33, 31–41.

Luque, L., Lario, J., Zazo, C., Goy, J.L., Dabrio, C.J., Silva, P.G., 2001. Tsunami deposits as paleoseismic indicators: examples from the Spanish coast. Acta geológica hispánica 36, 197–211.

Mansinha, L.A., Smylie, D.E., 1971. The displacement fields of inclined faults. Bull. Seismol. Soc. Am. 61, 1433–1440.

Martínez-Loriente S, Gràcia E, Bartolome R, Perea H, Klaeschen D, Dañobeitia JJ, Zitellini N, Wynn RB, Masson DG., 2018. Morphostructure, tectono-sedimentary evolution and seismic potential of the Horseshoe Fault, SW Iberian Margin. Basin Res 30:. https://doi.org/10.1111/bre.12225

Medina, F., Mhammdi, N., Chiguer, A., Akil, M., Jaaidi, E.B., 2011. The Rabat and Larache boulder fields; new examples of high-energy deposits related to storms and tsunami waves in north-western Morocco. Nat. Hazards 59, 725.

Mellas, S., Leone, F., Omira, R., Gherardi, M., Baptista, M.-A., Zourarah, B., Péroche, M., Lagahé, É., 2012. Le risque tsunamique au Maroc: modélisation et évaluation au moyen d'un premier jeu d'indicateurs d'exposition du littoral atlantique. Physio-Géo. Géographie Phys. Environ. 119–139.

Mhammdi, N., Medina, F., Kelletat, D., Ahmamou, M., Aloussi, L., 2008. Large boulders along the Rabat coast (Morocco); possible emplacement by the November, 1st, 1755 AD tsunami. Sci. Tsunami Hazards 27, 17–30.

Mhammdi N, Medina F., 2015. Recent tsunami deposits along the Moroccan Atlantic Coast. In: XIV Reunión Nacional de Cuaternario. Granada

Morton, R.A., Richmond, B.M., Jaffe, B.E., Gelfenbaum, G., 2008. Coarse-clast ridge complexes of the Caribbean: a preliminary basis for distinguishing tsunami and storm-wave origins. J. Sediment. Res. 78, 624–637.

Oliveira, M.A., Andrade, C., Freitas, M.C., Costa, P., Taborda, R., Janardo, C., Neves, R., 2011. Transport of large boulders quarried from shore platforms of the Portuguese west coast. J. Coast. Res. 1871–1875.

Omira, R., Baptista, M.A., Matias, L., Miranda, J.M., Catita, C., Carrilho, F., Toto, E., 2009. Design of a sea-level tsunami detection network for the Gulf of Cadiz. Nat. Hazards Earth Syst. Sci. 9, 1327–1338.

Omira, R., Baptista, M.A., Miranda, J.M., Toto, E., Catita, C., Catalao, J., 2010. Tsunami vulnerability assessment of Casablanca-Morocco using numerical modelling and GIS tools. Nat. hazards 54, 75–95.

Omira, R., Baptista, M.A., Miranda, J.M., 2011. Evaluating tsunami impact on the Gulf of Cadiz coast (Northeast Atlantic). Pure Appl. Geophys. 168, 1033–1043.

Omira, R., Baptista, M.A., Mellas, S., Leone, F., de Richemond, N.M., Zourarah, B., Cherel, J.-P., 2012. The November 1st, 1755 tsunami in Morocco: Can numerical modeling clarify the uncertainties of historical reports. Tsunami-Analysis a Hazard-From Phys. Interpret. to Hum. Impact. InTech 61–76.

Omira, R., Baptista, M.A., Matias, L., 2015. Probabilistic tsunami hazard in the Northeast Atlantic from near- and far-field tectonic sources. Pure Appl. Geophys. 172, 901–920.

Pro, C., Buforn, E., Bezzeghoud, M., Ud\'\ias, A., 2013. The earthquakes of 29 July 2003, 12 February 2007, and 17 December 2009 in the region of Cape Saint Vincent (SW Iberia) and their relation with the 1755 Lisbon earthquake. Tectonophysics 583, 16–27.

Roger, J., Baptista, M. A., Mosher, D., Hébert, H., & Sahal, A., 2010a. Tsunami impact on Newfoundland, Canada, due to far-field generated tsunamis: implications on hazard assessment. In Proceedings of the 9th US National and 10th Canadian Conference on Earthquake Engineering, Toronto, July (pp. 25-29).

Roger, J., Allgeyer, S., Hébert, H., Baptista, M. A., Loevenbruck, A., & Schindelé, F., 2010b. The 1755 Lisbon tsunami in Guadeloupe Archipelago: source sensitivity and investigation of resonance effects. The Open Oceanography Journal, 4 (1).

Roger, J., Baptista, M. A., Sahal, A., Accary, F., Allgeyer, S., & Hébert, H., 2011. The transoceanic 1755 Lisbon tsunami in Martinique. Pure and Applied Geophysics, 168(6), 1015-1031.

Ruiz, F., Pozo, M., González-Regalado, M. L., Rodríguez Vidal, J., Cáceres, L. M., Abad, M., & Arroyo, M., 2021. New Geological Evidence of the 1755 Lisbon Tsunami from the Rock of Gibraltar (Southern Iberian Peninsula). Minerals, 11(12), 1397.

Satake K., Okal E.A., Borrero J.C., 2007. Tsunami and its Hazard in the Indian and Pacific Oceans: Introduction. In: Satake K., Okal E.A., Borrero J.C. (eds) Tsunami and Its Hazards in the Indian and Pacific Oceans. Pageoph Topical Volumes. Birkhäuser Basel. https://doi.org/10.1007/978-3-7643-8364-0_1

Scheffers, A., 2002. Paleotsunami evidences from boulder deposits on Aruba, Curaçao and Bonaire. Sci. Tsunami Hazards 20, 26–37.

Scheffers, A., Kelletat, D., 2005. Tsunami relics on the coastal landscape west of Lisbon, Portugal. Sci. Tsunami Hazards 23, 3–16.

Scholz, CH., 1981. Scaling laws for large earthquakes; consequences for physical models. Bull Seismol Soc Am 72:1–14

Silva, S., Terrinha, P., Matias, L., Duarte, J.C., Roque, C., Ranero, C.R., Geissler, W.H., Zitellini, N., 2017. Micro-seismicity in the Gulf of Cadiz: Is there a link between micro-seismicity, high magnitude earthquakes and active faults? Tectonophysics 717, 226–241.

Solares, J.M.M., Arroyo, A.L., Mezcua, J., 1979. Isoseismal map of the 1755 Lisbon earthquake obtained from Spanish data. Tectonophysics 53, 301–313.

Soyris, M., 1755. Extrait d'une lettre de Maroc en date du 5 novembre 1755 : de Soyris à Guys. Archives N.

Switzer, A.D., Burston, J.M., 2010. Competing mechanisms for boulder deposition on the southeast Australian coast. Geomorphology 114, 42–54.

Tadibaght, A., Agharroud, K., Bounab, A., M'rini, E., Siame, L., El Kharim, Y., & El Ouaty, O., 2022. Quantitative risk assessment in El-Jadida (Northern Atlantic Coast of Morocco) for a tsunami scenario equivalent to that of the 1755 Lisbon earthquake. Environmental Earth Sciences, 81(5), 1-18.

Thiebot, E., Gutscher, M.-A., 2006. The Gibraltar Arc seismogenic zone (part 1): constraints on a shallow east dipping fault plane source for the 1755 Lisbon earthquake provided by seismic data, gravity and thermal modeling. Tectonophysics 426, 135–152.

Titov, V. V, 1999. Offshore forecasting of Alaska-Aleutian subduction zone tsunamis in Hawaii. NOAA Technical Memorandum, ERL PMEL-114, Seattle, Washington, 22 pp.

Whelan, F., Kelletat, D., 2005. Boulder deposits on the southern Spanish Atlantic coast: possible evidence for the 1755 AD Lisbon tsunami. Sci. Tsunami Hazards 23, 25–38.

Wynn, R.B., Masson, D.G., Stow, D.A., Weaver, P.P., 2000. The Northwest African slope apron: a modern analogue for deep-water systems with complex seafloor topography. Mar. Pet. Geol. 17, 253–265.

Zitellini, N., Chierici, F., Sartori, R., Torelli, L., 1999. The tectonic source of the 1755 Lisbon earthquake and tsunami. Ann. Geophys. 42.

Zitellini, N., Mendes, L.A., Cordoba, D., Danobeitia, J., Nicolich, R., Pellis, G., Ribeiro, A., Sartori, R., Torelli, L., Bartolome, R., others, 2001. Source of 1755 Lisbon earthquake and tsunami investigated. Eos, Trans. Am. Geophys. Union 82, 285–291.

Zitellini, N., Gràcia, E., Matias, L., Terrinha, P., Abreu, M.A., DeAlteriis, G., Henriet, J.P., Dañobeitia, J.J., Masson, D.G., Mulder, T., others, 2009. The quest for the Africa--Eurasia plate boundary west of the Strait of Gibraltar. Earth Planet. Sci. Lett. 280, 13–50.